

Experimental study of turbulent transport of nanoparticles in convective turbulence

I. Shimberg, O. Shriki, O. Shildkrot, N. Kleorin, A. Levy, and I. Rogachevskii

*The Pearlstone Center for Aeronautical Engineering Studies, Department of Mechanical Engineering,
Ben-Gurion University of the Negev, P.O.Box 653, Beer-Sheva 8410530, Israel*

(Dated: April 13, 2022)

We perform experimental study of turbulent transport of nanoparticles in convective turbulence with the Rayleigh number $\sim 10^8$ in the air flow. We measure temperature field in many locations by a temperature probe equipped with 11 E-thermocouples. Nanoparticles of the size ~ 70 nm in diameter are produced by Advanced Electrospray Aerosol Generator. To determine the number density of nanoparticles, we use Condensation Particle Counter. We demonstrate that the joint action of turbulent effects (which are important in the core flow) and molecular effects (which are essential near the boundaries of the chamber) results in an effective accumulation of nanoparticles at the cold wall of the chamber. The turbulent effects are characterised by turbulent diffusion and turbulent thermal diffusion of nanoparticles, while the molecular effects are described by the Brownian diffusion and thermophoresis, as well as the adhesion of nanoparticles at the cold wall of the chamber. In different experiments in convective turbulence in a chamber with the temperature difference ΔT between the bottom and top walls varying between $\Delta T = 29$ K to $\Delta T = 61$ K, we find that the mean number density of nanoparticles decreases exponentially in time. For instance, the characteristic decay time of the mean number density of nanoparticles varies from 12.8 min for $\Delta T = 61$ K to 24 min for $\Delta T = 29$ K. For better understanding of experimental results, we perform one-dimensional mean-field numerical simulations of the evolution of the mean number density of nanoparticles for conditions pertinent to the laboratory experiments. The obtained numerical results are in a good agreement with the experimental results.

I. INTRODUCTION

Turbulence [1–7] and the associated turbulent transport of particles [8–14] have been investigated systematically for more than a hundred years in theoretical, experimental and numerical studies. But some fundamental questions remain. It is well-known that turbulence results in a sharp increase of the effective diffusion coefficient [15]. In addition to turbulent diffusion, there are various turbulent effects resulting in formation of inhomogeneities in spatial distribution of particles.

In a non-stratified inhomogeneous turbulence, turbophoresis of particles due to a combined effect of particle inertia and inhomogeneity of turbulence, can occur [16–21]. Turbophoresis causes an appearance of the additional non-diffusive flux of inertial particles proportional to the mean particle velocity, $\mathbf{V}_{\text{turbo}} \propto -f_{\text{turbo}}(\text{St}, \text{Re}) \nabla \langle \mathbf{u} \rangle^2$, where \mathbf{u} is the turbulent fluid velocity, $\text{St} = \tau_p / \tau_\eta$ is the Stokes number, $\tau_\eta = \tau_0 / \text{Re}^{1/2}$ is the Kolmogorov viscous time, $\tau_p = m_p / (3\pi\rho\nu d)$ is the Stokes time for the small spherical particles of the diameter d and mass m_p , and ρ is the fluid density, $\text{Re} = \ell_0 u_0 / \nu$ is the fluid Reynolds number, u_0 is the characteristic turbulent velocity at the integral scale ℓ_0 of turbulent motions and ν is the kinematic fluid viscosity. Due to turbophoresis inertial particles are accumulated in the vicinity of the minimum of the turbulent intensity.

In a turbulent flow with a non-zero mean temperature gradient an additional turbulent flux of particles appears in the direction opposite to that of the mean temperature gradient [22, 23]. This phenomenon of turbulent thermal diffusion causes a non-diffusive turbulent flux of particles in the direction of the turbulent heat flux (opposite

to the mean temperature gradient). Turbulent thermal diffusion results in accumulation of particles in the vicinity of the mean temperature minimum which leads to the formation of inhomogeneous spatial distributions of the mean particle number density. Turbulent thermal diffusion has been intensively investigated analytically [24–29] using different theoretical approaches. This phenomenon has been detected in laboratory experiments for micron-size particles in air flows in oscillating grid turbulence [30–32] and in multi-fan produced turbulence [33]. Turbulent thermal diffusion has been also detected in direct numerical simulations [34] and observed in the atmospheric turbulence [35, 36]. This phenomenon has been also shown to be important in astrophysical turbulent flows [37].

In spite of intensive laboratory studies of turbulent thermal diffusion of micron-size particles, this effect has not yet been investigated for nanoparticles. To study turbulent thermal diffusion of nanoparticles, one need to take into account the dependence of the characteristic relaxation time of particles (the Stokes time) on the Knudsen number, $\text{Kn} = 2\lambda/d$ [11], where λ is the mean free path of molecules and d is the particle diameter. Note also that various aspects of transport of nanoparticles in turbulent fluid flows have been studied in a number of papers [38–46].

In the present paper, we discuss results of the experimental study of turbulent transport of nanoparticles in convective turbulence. The effect of turbulent thermal diffusion in the core flow and molecular thermophoresis nearby the cold boundary are main effects resulting in accumulation of nanoparticles nearby the cold wall. Our main goal is to understand how fast it is possible to accumulate nanoparticles nearby the cold wall of the chamber,

and how to control this process. The effect of nanoparticle accumulation depends on properties of the temperature stratified turbulence. To understand how to control nanoparticle accumulation, we perform measurements of temperature fields in many locations in the chamber and conduct the direct measurements of the number density of nanoparticles in the chamber. This allows us to determine the time-dependence of the mean number density of nanoparticles in the chamber. To understand the experimental results, we also perform one-dimensional mean-field numerical simulations of transport of nanoparticles for conditions pertinent to the laboratory experiments.

This paper is organized as follows. In Section II we discuss the physics of turbulent thermal diffusion and in Section III we outline the numerical setup for the mean-field numerical simulations of turbulent transport of nanoparticles. In Section IV we describe the experimental setup and measurements techniques. In Section V we discuss the experimental results and compare these results with those of the mean-field numerical simulations performed for conditions pertinent to the laboratory experiments. Finally, conclusions are drawn in Section VI.

II. TURBULENT THERMAL DIFFUSION

In this Section we discuss the physics of the phenomenon of turbulent thermal diffusion. The evolution of the number density $n(t, \mathbf{r})$ of small particles in a turbulent flow is determined by the convective diffusion equation,

$$\frac{\partial n}{\partial t} + \nabla \cdot (n \mathbf{U}_p) = -\nabla \cdot \mathbf{J}_M, \quad (1)$$

where \mathbf{U}_p is the particle velocity advected by a turbulent temperature stratified fluid flow, \mathbf{J}_M is the molecular flux of particles that is given by

$$\mathbf{J}_M = -D \left[\nabla n + k_t \frac{\nabla T}{T} + k_p \frac{\nabla P}{P} \right], \quad (2)$$

where T and P are the temperature and pressure of the surrounding fluid, respectively. The first term ($\propto \nabla n$) in the right-hand side of Eq. (2) for the molecular flux of particles, describes Brownian (molecular) diffusion of particles, the second term accounts for the molecular flux of particles which is driven by the fluid temperature gradient ∇T (thermophoresis for particles or molecular thermal diffusion for gases), and the third term determines the molecular flux of particles which is driven by the fluid pressure gradient ∇P (molecular barodiffusion). Here D is the coefficient of the Brownian diffusion, $k_t \propto n$ is the thermal diffusion ratio and Dk_t is the coefficient of thermal diffusion, $k_p \propto n$ is the barodiffusion ratio and Dk_p is the coefficient of barodiffusion.

In a turbulent flow, large-scale dynamics of particles is determined by the equation for the mean particle number density $\bar{n}(t, \mathbf{r})$:

$$\frac{\partial \bar{n}}{\partial t} + \nabla \cdot (\bar{n} \bar{\mathbf{U}}_p) = -\nabla \cdot (\bar{\mathbf{J}}_T + \bar{\mathbf{J}}_M), \quad (3)$$

where $\bar{\mathbf{U}}_p$ is the mean particle velocity, $\bar{\mathbf{J}}_M$ is the averaged molecular flux of particles,

$$\bar{\mathbf{J}}_M = -D \left[\nabla \bar{n} + k_t \frac{\nabla \bar{T}}{\bar{T}} + k_p \frac{\nabla \bar{P}}{\bar{P}} \right], \quad (4)$$

\bar{T} and \bar{P} are the mean fluid temperature and pressure, respectively, $\bar{\mathbf{J}}_T$ is the turbulent flux of particles [22, 23],

$$\bar{\mathbf{J}}_T = -D_T \left[\nabla \bar{n} + k_T \frac{\nabla \bar{T}}{\bar{T}} + k_P \frac{\nabla \bar{P}}{\bar{P}} \right]. \quad (5)$$

Here D_T is the coefficient of turbulent diffusion, $k_T = \bar{n} f_p(d, \text{Re}, \bar{T})$ can be interpreted as the turbulent thermal diffusion ratio and $D_T k_T$ is the coefficient of turbulent thermal diffusion, $k_P = -\bar{n}$ can be interpreted as the turbulent barodiffusion ratio and $D_T k_P$ is the coefficient of turbulent barodiffusion, $f_p(d, \text{Re}, \bar{T})$ is the function which depends on the particle diameter, the Reynolds number and the mean fluid temperature [28].

The physics of the effect of turbulent thermal diffusion for solid particles $\rho_p \gg \rho$ is as follows [22, 23], where ρ_p is the material density of the particles. The inertia causes particles inside the turbulent eddies to drift out to the boundary regions between eddies due to the centrifugal inertial force. Indeed, for large Péclet numbers, when molecular diffusion of particles in Eq. (1) can be neglected, we obtain that $\nabla \cdot \mathbf{U}_p \approx -n^{-1} dn/dt$. On the other hand, for inertial particles, $\nabla \cdot \mathbf{U}_p = (\tau_p/\rho) \nabla^2 P$ [22]. Therefore, in regions with maximum fluid pressure fluctuations (where $\nabla^2 p < 0$), there is accumulation of inertial particles, i.e., $dn'/dt \propto -\bar{n} (\tau_p/\bar{p}) \nabla^2 p > 0$. These regions have low vorticity and high strain rate. Here n' and p are fluctuations of particle number density and fluid pressure, respectively, and \bar{p} is the mean density of the surrounding fluid. Similarly, there is an outflow of inertial particles from regions with minimum fluid pressure fluctuations.

In homogeneous and isotropic turbulence with a zero gradient of the mean temperature, there is no preferential direction, so that there is no large-scale effect of particle accumulation, and the pressure (temperature) of the surrounding fluid is not correlated with the turbulent velocity field. The only non-zero correlation is $\langle (\mathbf{u} \cdot \nabla) p \rangle$, which contributes to the flux of the turbulent kinetic energy density.

In temperature-stratified turbulence, fluctuations of fluid temperature θ and velocity \mathbf{u} are correlated due to a non-zero turbulent heat flux, $\langle \theta \mathbf{u} \rangle \neq \mathbf{0}$. Fluctuations of temperature cause pressure fluctuations, which result in fluctuations of the number density of particles. Note that in the mechanism of turbulent thermal diffusion, only pressure fluctuations which are correlated with velocity fluctuations due to a non-zero turbulent heat flux play a crucial role. Increase of the fluid pressure fluctuations is accompanied by an accumulation of particles, and the direction of the mean flux of particles coincides with that of the turbulent heat flux. The turbulent flux

of particles is directed to the minimum of the mean temperature, and the particles tend to be accumulated in this region [14].

The similar effect of accumulation of particles in the vicinity of the mean temperature minimum and the formation of inhomogeneous spatial distributions of the mean particle number density exists also for non-inertial particles or gaseous admixtures in turbulent compressible flows [23, 29, 34]. Compressibility in a low-Mach-number stratified turbulent fluid flow [with $\nabla \cdot \mathbf{u} \approx -(\mathbf{u} \cdot \nabla \bar{\rho})/\bar{\rho} \neq 0$] causes an additional non-diffusive component of the turbulent flux of non-inertial particles or gases, and results in the formation of large-scale inhomogeneous structures in spatial distributions of non-inertial particles. In a temperature stratified turbulence, preferential concentration of particles caused by turbulent thermal diffusion can occur in the vicinity of the minimum of the mean temperature. The latter effect is caused by the compressibility of the turbulent fluid flow [$\nabla \cdot \mathbf{u} \propto (\mathbf{u} \cdot \nabla \bar{T})/\bar{T} \neq 0$]. This effect plays an important role in the dynamics of gaseous pollutants in the stratified atmospheric turbulence.

III. SETUP FOR MEAN-FIELD NUMERICAL SIMULATIONS

For better understanding of the experimental results obtained in this study, we perform one-dimensional mean-field numerical simulations of turbulent transport of nanoparticles for the conditions pertinent to the laboratory experiments. In particular, we study the evolution of the mean number density of nanoparticles, $\bar{n}(t, z)$, by solving numerically the evolutionary equation for the mean number density of nanoparticles:

$$\frac{\partial \bar{n}}{\partial t} + \nabla_z \left[\left(V_z^{(\text{eff})} + V_z^{(\text{tp})} \right) \bar{n} - (D + D_T) \nabla_z \bar{n} \right] = 0. \quad (6)$$

This equation takes into account the total transport effective velocity $\mathbf{V}^{(\text{eff})} + \mathbf{V}^{(\text{tp})}$ due to turbulent thermal diffusion and thermophoresis, where $\mathbf{V}^{(\text{eff})}$ is the effective pumping velocity caused by turbulent thermal diffusion and $\mathbf{V}^{(\text{tp})}$ is the thermophoretic velocity (see below). This equation also takes into account the total particle diffusion $D + D_T$, where D is the coefficient of the Brownian diffusion, $D_T = u_0 \ell_0/3$ is the coefficient of turbulent diffusion and u_0 is the characteristic turbulent velocity at the integral turbulence scale ℓ_0 . In the one-dimensional mean-field numerical simulations, we have not taken into account the mean velocity field of the large-scale circulation produced in a small-scale convective turbulence.

Turbulent thermal diffusion is described in terms of the effective pumping velocity $\mathbf{V}^{(\text{eff})}$ resulting in non-diffusive turbulent particle flux, $\bar{n} \mathbf{V}^{(\text{eff})}$. The effective pumping velocity caused by turbulent thermal diffusion

of nanoparticles is given by

$$\mathbf{V}^{(\text{eff})} = -D_T \alpha(d, \text{Kn}, \text{Re}) \frac{\nabla \bar{T}}{\bar{T}}, \quad (7)$$

where

$$\alpha(d, \text{Kn}, \text{Re}, \bar{T}) = 1 + \frac{\tau_p(d, \text{Kn})}{\tau_0} \text{Re}^{1/4} \ln(\text{Re}) \left(\frac{L_{\text{eff}}}{\ell_0} \right), \quad (8)$$

(see [19, 35, 47]), where $L_{\text{eff}} = 2c_s^2 \tau_\eta^{3/2}/3\nu^{1/2}$ is the effective length scale, c_s is the sound speed, $\tau_p = m_p C_c/(3\pi\rho\nu d)$ is the Stokes time for nanoparticles and $C_c = 1 + \text{Kn}[1.257 + 0.4 \exp(-1.1\text{Kn})]$ is the slip correction factor [48]. For instance, $C_c = 4.95$ for $d = 50$ nm, $C_c = 3.7$ for $d = 70$ nm and $C_c = 2.85$ for $d = 100$ nm [11].

In turbulent flows, at the vicinity of the boundaries where the intensity of velocity fluctuations drastically decreases, the molecular effects (e.g, molecular diffusion and thermophoresis) become more important than the turbulent effects. The thermophoretic velocity can be estimated as $V^{(\text{tp})} = -f_{\text{tp}} \nu \nabla \bar{T}/\bar{T}$, where f_{tp} is a function of Knudsen number, the particle size and the ratio of the heat conductivities of the particle and the fluid. For small particles (i.e for large Knudsen numbers, $\text{Kn} \gg 1$), the coefficient $f_{\text{tp}} = 3/4$ for mirror rebound of the gas molecules from the particles and $f_{\text{tp}} = 1/2$ for diffuse evaporation of the molecules when they "forget" the direction and value of their velocity prior to the impact [49]. Different aspects related to molecular effects have been studied in a number of publications [50–53].

In the mean-field numerical simulations, we use the following boundary conditions:

- at the bottom boundary ($z = 0$), the total flux of particles,

$$F_z^{(n)} = \left(V_z^{(\text{eff})} + V_z^{(\text{tp})} \right) \bar{n} - (D + D_T) \nabla_z \bar{n}, \quad (9)$$

vanishes;

- at the upper boundary ($z = L_z$), the vertical gradient of the mean number density of nanoparticles $\nabla_z \bar{n}$ vanishes. The latter condition implies that all particles in the vicinity of the cold wall of the chamber (the upper boundary) are trapped due to adhesion of particles at the wall.

The total transport effective velocity $\mathbf{V}^{(\text{eff})} + \mathbf{V}^{(\text{tp})}$ caused by turbulent thermal diffusion and thermophoresis, depend on the vertical profile of the mean temperature. We determine semi-analytically the vertical profile of the mean temperature. To this end, we take into account that the vertical component of the turbulent heat flux is $F_z = \langle u_z \theta \rangle = -\kappa_T \nabla_z \bar{T}$, where $\kappa_T = \ell_z u_z^{(\text{rms})} = (2\ell_z^4 \beta F_z)^{1/3}$ is the turbulent heat conductivity, $\beta = g/T_*$ is the buoyancy parameter, \mathbf{g} is the gravity acceleration, T_* is the characteristic temperature

in the basic reference state, and ℓ_z is the vertical integral turbulent scale. We take into account that in convective turbulence, the characteristic vertical turbulent velocity is $u_z^{(\text{rms})} = (2\ell_z\beta F_z)^{1/3}$. The latter equation follows from the steady-state solution of the budget equation for the turbulent kinetic energy, which allows us to relate the turbulent velocity with the turbulent heat flux. Next, we use the following model for the vertical integral length scale: in the core flow (for $z_* \leq z \leq L_z - z_*$), the vertical integral length is $\ell_z = \ell_0$; and near the bottom and top boundaries where the intensity of turbulence vanishes, the vertical integral length is $\ell_z = \ell_0 \phi(z)$. Here L_z is the thickness of the convective layer (the vertical height of the chamber), $z_* = \epsilon L_z$ with $\epsilon \ll 1$ and $\phi(z)$ is the rapidly decreasing smooth function that varies from 1 to 0.

At the vicinity of the boundaries the molecular diffusion of the mean temperature is taking into account, so that the total vertical heat flux $F_z^{(\text{tot})}$ is the sum of turbulent, $-\kappa_T \nabla_z \bar{T}$, and molecular, $-\kappa \nabla_z \bar{T}$, vertical heat fluxes, i.e., $F_z^{(\text{tot})} = -(\kappa_T + \kappa) \nabla_z \bar{T}$, where κ is the molecular temperature diffusivity. The latter equation can be reduced to a cubic equation $KM^3 + M^2 - K = 0$ for $M = (F_z/F_z^{(\text{tot})})^{1/3}$, where $K = \kappa^{-1} (2\ell_z^4 \beta F_z^{(\text{tot})})^{1/3}$. Numerical solution of this cubic equation allows us to obtain the vertical profile for the mean temperature. This vertical profile of the mean temperature is used to determine the total transport effective velocity $\mathbf{V}^{(\text{eff})} + \mathbf{V}^{(\text{tp})}$ caused by turbulent thermal diffusion and thermophoresis in the mean-field numerical simulations of nanoparticles in convective turbulence for the conditions pertinent to the laboratory experiments. The numerical simulations are performed using the Matlab. The numerical results will be compared with the experimental results (see Section V).

IV. EXPERIMENTAL SETUP

We conduct various sets of experiments in a temperature stratified convective turbulence. The experimental setup with an isolated chamber is designed for measurements of spatial distributions of the fluid temperature and the number density of nanoparticles in turbulent convection (see Figs. 1–2). The chamber is fully isolated using high-quality glass, and there is also control humidity in the chamber.

The experiments are conducted with air as the working fluid in a rectangular chamber with dimensions $L_x \times L_y \times L_z$, where $L_x = L_z = 20$ cm, $L_y = 50$ cm and the z axis is in the vertical direction (see Fig. 1, bottom panel). A vertical mean temperature gradient in the turbulent air flow is formed by attaching two aluminium heat exchangers to the bottom and top walls of the test section (a heated bottom and a cooled top wall of the chamber). A thickness of the massive aluminium heat exchangers is 2 cm. The top plate is a bottom wall of the

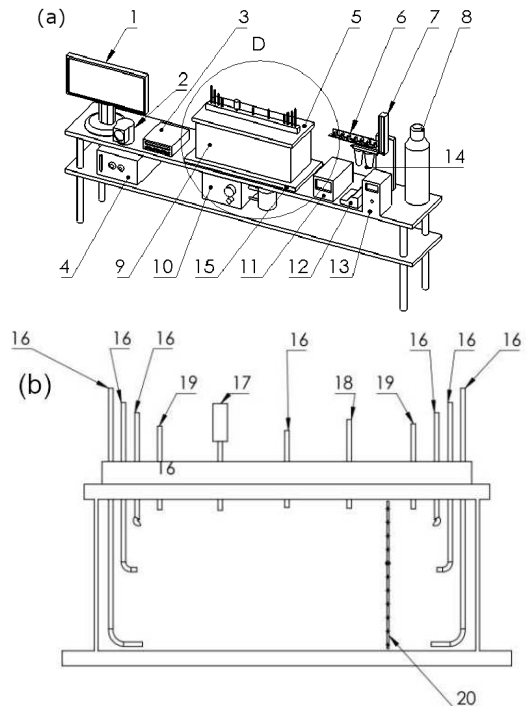


FIG. 1. A scheme of the experimental set-up: (a). Upper panel: (1) display; (2) pressure measurements device; (3) data collection for temperature and humidity measurements; (4) computer; (5) cooler plate; (6-7) controllers for nanoparticle number density measurements; (8) container for CO_2 for nanoparticles generator; (9) chamber (see also the bottom panel); (10) cooling system; (11) nanoparticles generator; (12) spray for nanoparticles generator; (13) condensation particle counter; (14) air quality controller nanoparticles generator; (15) heating system. (b). Bottom panel: (16) probes for nanoparticle number density measurements; (17) probe for humidity measurements; (18) probe for pressure measurements; (19) air supply tube; (20) probes for temperature measurements.

tank with cooling water. Cold water is pumped into the cooling system through two inlets and flows out through two outlets located at the side wall of the cooling system. The bottom plate is attached to the electrical heater with wire tightly laid in the grooves milled in the aluminum plate and provided uniform heating. Energy supplied to the heater is varied in order to obtain necessary temperature difference between heater and cooler. Characteristic time of heater is approximately 180 min that stabilize applied temperature during measurements.

The temperature field is measured with a temperature probe equipped with 11 E-thermocouples (with the diameter of 0.13 mm and the sensitivity of $\approx 65 \mu\text{V/K}$) attached to a rod with a diameter 4 mm (see Fig. 1, bottom panel). The spacing between thermocouples along the rod can be changed from 10 to 20 mm. Each thermocouple is inserted into a 1 mm diameter and 45 mm long case. A tip of a thermocouple protruded at the length of 15 mm out of the case. Thermocouples of type E are

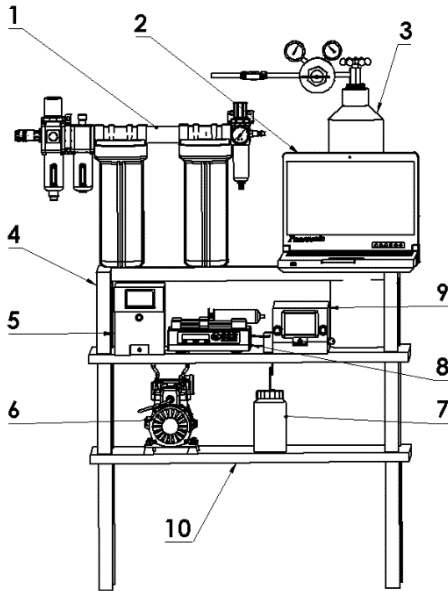


FIG. 2. A scheme of the experimental set-up: (1) air filter and dryer for particles generator; (2) display; (3) gas cylinder CO_2 for particles generator; (4) frame; (5) particles counter; (6) vacuum pump of particles counter; (7) butanol waste container (drain balun of counter); (8) particles supply pump; (9) particles generator; (10) frame.

used for the temperature measurements in the core flow, while thermocouples of type K are used for temperature measurements at the heater and the cooler. All thermocouples are built by a manufacturer. Calibrations of all E-thermocouples in the temperature probe is performed for three experiments with boiled water ($T = 373$ K), the cold water with ice ($T = 273$ K) and water with intermediate temperature ($T = 296$ K). Comparisons is performed using a precision temperature measurement manufactured device.

The temperature is measured for 11 rod positions with 10-20 mm intervals in the horizontal direction. A sequence of 240 temperature readings for every thermocouple at every rod position is recorded and processed. We measure the temperature field in many locations. Performing direct continuous measurements of the temperatures at the cooled top surface and at the heated bottom surface and using a standard device for supporting constant temperature difference ΔT between the top and bottom surfaces (Contact voltage regulator TDGC-2K), we control the constant temperature difference ΔT during the experiments.

Similar measurement techniques and data processing procedure have been used by us previously in the experimental study of different aspects of turbulent convection and stably stratified turbulence [54–57], investigations of turbulent thermal diffusion [22–25] of micron-size particles in the oscillating grid turbulence [28, 30–32] and in turbulence produced by the multi-fan generator [33], and investigations of small-scale particle clustering [47, 58, 59]

in the oscillating grid turbulence [60].

To study turbulent thermal diffusion in the experiments we use 70 nm nanoparticles produced by Advanced Electro Spray Aerosol Generator (Model 3482). To determine the number density of nanoparticles, we use Condensation Particle Counter (Model 3750). We conduct experiments for different temperature differences (from $\Delta T = 29$ K up to $\Delta T = 61$ K) between the top and bottom walls as well as for isothermal flow. The particle number density measurements are performed for three heights z and two horizontal coordinates y .

V. RESULTS

Let us discuss the obtained results. In Fig. 3 we show the patterns of the mean temperature field \bar{T} in the yz plane obtained in the laboratory experiments for different temperature differences ΔT between the bottom and upper walls of the chamber: $\Delta T = 29$ K (upper panel); $\Delta T = 44$ K (middle panel); $\Delta T = 61$ K (bottom panel). Figure 3 indicates that there are two large-scale circulations in the experiments for $\Delta T = 29$ K and $\Delta T = 44$ K, and one large-scale circulation for $\Delta T = 61$ K. The Rayleigh number $\text{Ra} = \alpha_* g L_z^3 \Delta T / (\nu \kappa)$ in the experiments varies in the interval $\text{Ra} = (0.61 - 1.23) \times 10^8$ depending on the different temperature differences ΔT between the bottom and upper walls of the chamber, where α_* is the thermal expansion coefficient and L_z is the height of the chamber.

In the present study we have not performed measurements of the velocity field. The velocity field in turbulent convection in a similar experimental setup has been investigated in our previous study [54], where we have determined the mean and turbulent velocity fields, the integral scales of turbulence in the horizontal and vertical directions, the rates of energy dissipation and production in the convective turbulence, the dependencies of these turbulent parameters on the values of the temperature difference between the bottom and top walls of the chamber. For instance, the integral turbulence scales in the chamber with convective turbulence are $\ell_x = \ell_z = 3$ cm, $\ell_y = 5$ cm, the characteristic vertical turbulent velocity is $u_z = 5$ cm/s at $\Delta T = 60$ K that depends on ΔT as $u_z \propto (\Delta T)^{1/2}$ [54].

In Figs. 4 and 5 we also plot vertical profiles of the mean temperature \bar{T} and the vertical gradient $\nabla_z \bar{T}$ of the mean temperature obtained in the laboratory experiments for different temperature differences ΔT between the bottom and upper walls of the chamber. These profiles of the mean temperature \bar{T} are compared with the results of the semi-analytical mean-field calculations described at the end of Section III. Figures 4 and 5 show that there is a qualitative agreement between the modelling and experimental results. As usual, the strong temperature gradient is located near the walls of the chamber, while inside the large-scale circulations the vertical gradient $\nabla_z \bar{T}$ of the mean temperature is much

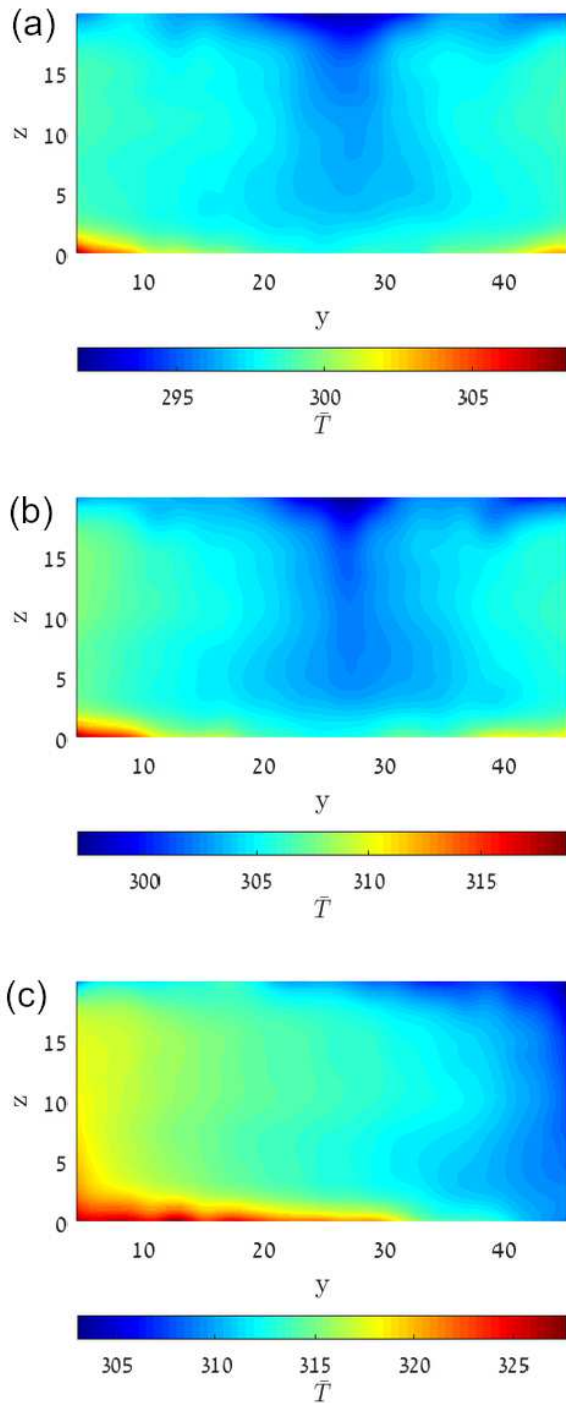


FIG. 3. Patterns of the mean temperature field \bar{T} in the yz plane obtained in the laboratory experiments for different temperature differences ΔT between the bottom and upper walls of the chamber: (a) $\Delta T = 29$ K (upper panel); (b) $\Delta T = 44$ K (middle panel); (c) $\Delta T = 61$ K (bottom panel). The coordinates are measured in cm and temperature is measured in K.

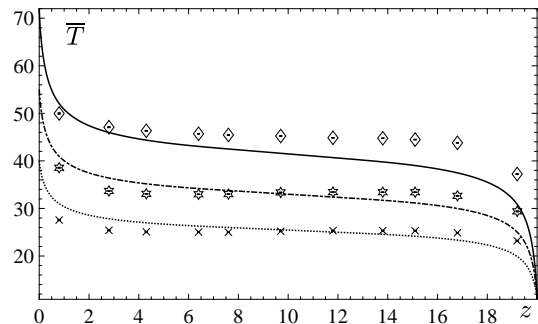


FIG. 4. Comparison of vertical profiles of the mean temperature \bar{T} obtained in the laboratory experiments for different temperature differences ΔT between the bottom and upper walls of the chamber: $\Delta T = 29$ K (slanting crosses); $\Delta T = 44$ K (stars); $\Delta T = 61$ K (diamonds); and in the semi-analytical mean-field calculations: $\Delta T = 29$ K (dotted line); $\Delta T = 44$ K (dashed line); $\Delta T = 61$ K (solid line). The coordinate z is measured in cm and the mean temperature in C.

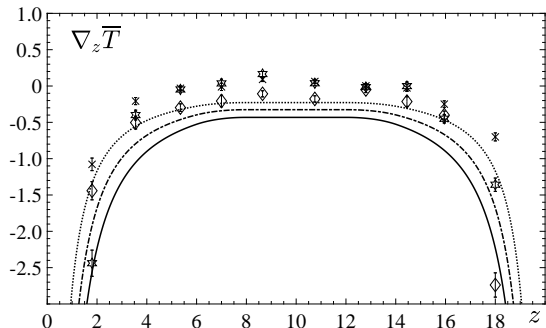


FIG. 5. Comparison of vertical profiles of the vertical mean temperature gradient $\nabla_z \bar{T}$ obtained in the laboratory experiments for different temperature differences ΔT between the bottom and upper walls of the chamber: $\Delta T = 29$ K (slanting crosses); $\Delta T = 44$ K (stars); $\Delta T = 61$ K (diamonds); and in the semi-analytical mean-field calculations: $\Delta T = 29$ K (dotted line); $\Delta T = 44$ K (dashed line); $\Delta T = 61$ K (solid line). The coordinate z is measured in cm and the mean temperature gradient $\nabla_z \bar{T}$ is measured in K/cm.

weaker. The main reason for the deviations of the modelling and experimental results for the temperature field is that in the one-dimensional semi-analytical calculations of the vertical mean temperature distribution, we have not taken into account the mean velocity field of the large-scale circulation. We have checked that a particular form of the decreasing smooth function $\phi(z)$ that describes the spatial vertical profile of the integral turbulence scale in the region where turbulent intensity strongly decreases, weakly affects the mean temperature distribution. Note also that we have not performed temperature measurements in the vicinity of the wall, but measure temperature at the heat exchangers and in the core flow.

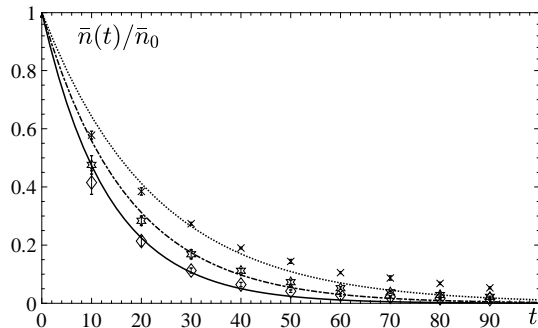


FIG. 6. Comparison of the time evolution of the normalized mean number density of nanoparticles $\bar{n}(t)/\bar{n}_0$ obtained in the laboratory experiments for different temperature differences ΔT between the bottom and upper walls of the chamber: $\Delta T = 29$ K (slanting crosses); $\Delta T = 44$ K (stars); $\Delta T = 61$ K (diamonds); and in the mean-field simulations: $\Delta T = 29$ K (dotted line); $\Delta T = 44$ K (dashed line); $\Delta T = 61$ K (solid line). Here $\bar{n}(t) = L_z^{-1} \int_0^{L_z} \bar{n}(t, z) dz$ and $\bar{n}_0 = \bar{n}(t = 0)$. The time is measured in minutes.

Measurements of number density of nanoparticles allow us to determine the time evolution of the normalized mean number density $\bar{n}(t)/\bar{n}_0$ of nanoparticles obtained in the laboratory experiments for different temperature differences ΔT between the bottom and upper walls of the chamber (see Fig. 6). Here $\bar{n}(t) = L_z^{-1} \int_0^{L_z} \bar{n}(t, z) dz$ is the mean number density of nanoparticles averaged over the vertical coordinate z and $\bar{n}_0 = \bar{n}(t = 0)$. Inspection of Fig. 6 shows that in the experiments with turbulent convection with different temperature difference between the bottom and top walls of the chamber, the mean number density of nanoparticles decreases exponentially in time. The characteristic decay time of the mean number density of nanoparticles varies from 12.8 min for the temperature difference $\Delta T = 61$ K, to 16.3 min for $\Delta T = 44$ K and to 24 min for $\Delta T = 29$ K.

We also perform comparison of the obtained experimental results with the results of the mean-field numerical simulations of transport of nanoparticles which accounts for molecular and turbulent effects for the conditions pertinent to the laboratory experiments. The numerical setup is described in Section III. As follows from Fig. 6, the obtained numerical results related to the time evolution of the normalized mean number density of particles $\bar{n}(t)/\bar{n}_0$ are in an agreement with the results of the laboratory experiments.

In Fig. 7 we show the time evolution of the ratios of the mean number densities of nanoparticles $\bar{n}_{\text{bottom}}/\bar{n}_{\text{top}}$ and $\bar{n}_{\text{middle}}/\bar{n}_{\text{top}}$ obtained in the laboratory experiments for the temperature difference $\Delta T = 61$ K between the bottom and top walls of the chamber, where \bar{n}_{top} , \bar{n}_{bottom} and \bar{n}_{middle} are the mean number densities of nanoparticles measured in the vicinity of the top, bottom and middle parts of the chamber, respectively. Figure 7 demonstrates that the distribution of the mean number den-

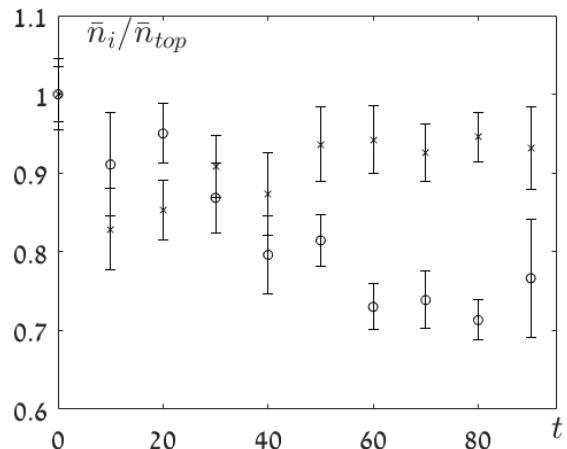


FIG. 7. The time evolution of the ratios of the mean number densities of nanoparticles $\bar{n}_{\text{bottom}}/\bar{n}_{\text{top}}$ (slanting crosses) and $\bar{n}_{\text{middle}}/\bar{n}_{\text{top}}$ (circles) obtained in the laboratory experiments for the temperature difference $\Delta T = 61$ K between the bottom and top walls of the chamber, where \bar{n}_{top} , $\bar{n}_i = \bar{n}_{\text{bottom}}$ and $\bar{n}_i = \bar{n}_{\text{middle}}$ are the mean number densities of nanoparticles measured at the top, bottom and middle parts of the chamber, respectively. The time is measured in minutes.

sity of nanoparticles is inhomogeneous. In particular, the maximum mean number density of nanoparticles is located near the top cold wall of the chamber, i.e. for $t > 0$, the ratios $\bar{n}_{\text{bottom}}/\bar{n}_{\text{top}}$ and $\bar{n}_{\text{middle}}/\bar{n}_{\text{top}}$ are always less than 1.

Let us estimate the effective pumping velocity caused by turbulent thermal diffusion of nanoparticles, the velocity due to the thermophoresis and the terminal fall velocity. The effective pumping velocity caused by turbulent thermal diffusion of nanoparticles having the diameter $d = 70$ nm, is 7×10^{-2} cm/s, where we use Eqs. (7)–(8). We also take into account that the value of the gradient of the mean temperature measured in the core flow at $3 \leq z \leq 17$ cm is $\nabla_z \bar{T} = 0.4$ K/cm (see Fig. 5). In this region the turbulent effects (turbulent thermal diffusion and turbulent diffusion) are dominant. Now we estimate the terminal fall velocity $V_g = \tau_p g = 3 \times 10^{-5}$ cm/s, where $\tau_p = 3 \times 10^{-8}$ s is the Stokes time for nanoparticles with the diameter $d = 70$ nm. The velocity due to the thermophoresis in the vicinity of the cold wall, is about $V^{(\text{tp})} = 1.2 \times 10^{-3}$ cm/s at $z = 1.6$ cm, where the gradient of the mean temperature is 3 K/cm.

Note that several different mechanisms affect the particle transport: the mean fluid velocity of the large-scale circulations, turbulent diffusion, turbulent thermal diffusion, Brownian motions and thermophoresis. The mean fluid velocity of the large-scale circulations causes mixing of nanoparticles in the chamber producing nearly homogeneous distribution of nanoparticles in the chamber. Since the mean fluid velocity in the downdrafts and updrafts inside the large-scale circulations have opposite directions, the total vertical transport of nanoparticles

(averaged over the horizontal plane) due to the mean velocity is negligible and it cannot cause the particle accumulation in the vicinity of the cold wall of the chamber. On the other hand, the effective pumping velocity caused by turbulent thermal diffusion, is the vertical velocity directed to the cold wall of the chamber (it is proportional to $-\nabla\bar{T}$). The effective pumping velocity results in an inhomogeneous distribution of nanoparticles where particles tend to be accumulated in the vicinity of the cold wall of the chamber. However, turbulent thermal diffusion is a turbulent effect and it vanishes near the walls whereby the intensity of turbulence tends to zero. On the other hand, in the vicinity of the walls, the molecular effects (mainly the thermophoresis and adhesion of nanoparticles) play a crucial role in the particle accumulation at the cold wall of the chamber. Indeed, the thermophoretic velocity is proportional to $-\nabla\bar{T}$, and the mean temperature gradient is maximum in the vicinity of the walls. Therefore, the thermophoretic velocity finally causes the trapping of particles by the cold wall of the chamber.

VI. DISCUSSION AND CONCLUSIONS

We have performed different sets of experiments with turbulent convection to study turbulent transport of nanoparticles. The temperature field has been measured with a temperature probe equipped with 11 E-thermocouples. To determine the number density of nanoparticles, we used Condensation Particle Counter. Nanoparticles of 70 nm in diameter are produced by Advanced Electrospray Aerosol Generator. We measure the number density of nanoparticles as a function of time in 3 locations in vertical directions. In the different experiments with turbulent convection with the temperature difference between the bottom and top walls of the chamber ΔT varying between $\Delta T = 29$ K to $\Delta T = 61$ K, it has been shown that the mean number density of nanoparticles decreases exponentially in time. For instance, the characteristic decay time of the mean number density of

nanoparticles varies from 12.8 min for the temperature difference between the bottom and top walls of the chamber $\Delta T = 61$ K, to 16.3 min for $\Delta T = 44$ K and to 24 min for $\Delta T = 29$ K. The main reasons for this effect are as follows.

- The large-scale circulations in convective turbulence cause mixing of nanoparticles in the chamber.
- The effective pumping velocity due to turbulent thermal diffusion in the core flow results in the drift of nanoparticles to the cold wall of the chamber.
- The thermophoresis and adhesion of nanoparticles in the vicinity of the cold wall of the chamber where the mean temperature gradient is enough strong, result in trapping of nanoparticles by the cold wall.

We have also performed one-dimensional mean-field numerical simulations of the evolution of the mean number density of nanoparticles which take into account turbulent and molecular effects. The molecular effects include the Brownian diffusion of nanoparticles, the thermophoresis, and the adhesion of nanoparticles at the cold surfaces. The turbulent effects are described by turbulent diffusion and turbulent thermal diffusion of nanoparticles. These simulations allow us to determine the time-dependence of the mean number density of nanoparticles and to find the characteristic decay time of the mean concentration of nanoparticles. The obtained numerical results are in an agreement with the experimental results.

ACKNOWLEDGMENTS

This research was supported in part by the Israel Ministry of Science and Technology (grant No. 3-16516).

DATA AVAILABILITY

The data that support the findings of this study are available from the corresponding author upon reasonable request.

-
- [1] A. S. Monin and A. M. Yaglom, *Statistical Fluid Mechanics* (MIT Press, Cambridge, Massachusetts, 1971), v. 1.
 - [2] A. S. Monin and A. M. Yaglom, *Statistical Fluid Mechanics* (MIT Press, Cambridge, Massachusetts, 1975), v. 2.
 - [3] W. D. McComb, *The Physics of Fluid Turbulence* (Oxford Science Publ., Oxford, 1990).
 - [4] U. Frisch, *Turbulence: the Legacy of A. N. Kolmogorov* (Cambridge University Press, Cambridge, 1995).
 - [5] S. B. Pope, *Turbulent Flows* (Cambridge University Press, Cambridge, 2000).
 - [6] M. Lesieur, *Turbulence in Fluids* (Springer, Dordrecht, 2008).
 - [7] P. A. Davidson, *Turbulence in Rotating, Stratified and Electrically Conducting Fluids* (Cambridge University Press, Cambridge, 2013).
 - [8] G. T. Csanady, *Turbulent Diffusion in the Environment* (Reidel, Dordrecht, 1980).
 - [9] Ya. B. Zeldovich, A. A. Ruzmaikin, and D. D. Sokoloff, *The Almighty Chance* (Word Scientific Publ., Singapore, 1990).
 - [10] A. K. Blackadar, *Turbulence and Diffusion in the Atmosphere* (Springer, Berlin, 1997).
 - [11] J. H. Seinfeld and S. N. Pandis, *Atmospheric Chemistry and Physics. From Air Pollution to Climate Change.*, 2nd ed. (John Wiley & Sons, NY, 2006).
 - [12] L. I. Zaichik, V. M. Alipchenkov, and E. G. Sinaiski,

- Particles in turbulent flows (John Wiley & Sons, NY, 2008).
- [13] C. T. Crowe, J. D. Schwarzkopf, M. Sommerfeld and Y. Tsuji, *Multiphase flows with droplets and particles*, second edition (CRC Press LLC, NY, 2011).
- [14] I. Rogachevskii, *Introduction to Turbulent Transport of Particles, Temperature and Magnetic Fields* (Cambridge University Press, Cambridge, 2021).
- [15] G. I. Taylor, Diffusion by continuous movements. *Proc. London Math. Soc.* **2**, 196 (1922).
- [16] M. Caporaloni, F. Tampieri, F. Trombetti and O. Vittori, Transfer of particles in nonisotropic air turbulence, *J. Atmosph. Sci.* **32**, 565 (1975).
- [17] M. Reeks, The transport of discrete particle in inhomogeneous turbulence, *J. Aerosol Sci.* **14**, 729 (1983).
- [18] A. Guha, A unified Eulerian theory of turbulent deposition to smooth and rough surfaces, *J. Aerosol Sci.* **28**, 1517 (1997).
- [19] T. Elperin, N. Kleeorin and I. Rogachevskii, Formation of inhomogeneities in two-phase low-Mach-number compressible turbulent fluid flows, *Int. J. Multiphase Flow* **24**, 1163 (1998).
- [20] A. Guha, Transport and deposition of particles in turbulent and laminar flow, *Annu. Rev. Fluid Mech.* **40**, 311 (2008).
- [21] Dh. Mitra, N. E. L. Haugen and I. Rogachevskii, Turbophoresis in forced inhomogeneous turbulence, *Europ. Phys. J. Plus* **133**, 35 (2018).
- [22] T. Elperin, N. Kleeorin and I. Rogachevskii, Turbulent thermal diffusion of small inertial particles, *Phys. Rev. Lett.* **76**, 224 (1996).
- [23] T. Elperin, N. Kleeorin and I. Rogachevskii, Turbulent barodiffusion, turbulent thermal diffusion and large-scale instability in gases, *Phys. Rev. E* **55**, 2713 (1997).
- [24] T. Elperin, N. Kleeorin, I. Rogachevskii and D. Sokoloff, Passive scalar transport in a random flow with a finite renewal time: Mean-field equations, *Phys. Rev. E* **61**, 2617 (2000).
- [25] T. Elperin, N. Kleeorin, I. Rogachevskii and D. Sokoloff, Mean-field theory for a passive scalar advected by a turbulent velocity field with a random renewal time, *Phys. Rev. E* **64**, 026304 (2001).
- [26] R. V. R. Pandya and F. Mashayek, Turbulent thermal diffusion and barodiffusion of passive scalar and dispersed phase of particles in turbulent flows, *Phys. Rev. Lett.* **88**, 044501 (2002).
- [27] M. W. Reeks, On model equations for particle dispersion in inhomogeneous turbulence, *Int. J. Multiph. Flow* **31**, 93 (2005).
- [28] G. Amir, N. Bar, A. Eidelman, T. Elperin, N. Kleeorin, and I. Rogachevskii, Turbulent thermal diffusion in strongly stratified turbulence: Theory and experiments, *Phys. Rev. Fluids* **2**, 064605 (2017).
- [29] I. Rogachevskii, N. Kleeorin and A. Brandenburg, Compressibility in turbulent magnetohydrodynamics and passive scalar transport: mean-field theory, *J. Plasma Phys.* **84**, 735840502 (2018).
- [30] J. Buchholz, A. Eidelman, T. Elperin, G. Grünefeld, N. Kleeorin, A. Krein, I. Rogachevskii, Experimental study of turbulent thermal diffusion in oscillating grids turbulence, *Experim. Fluids* **36**, 879 (2004).
- [31] A. Eidelman, T. Elperin, N. Kleeorin, A. Krein, I. Rogachevskii, J. Buchholz, and G. Grünefeld, Turbulent thermal diffusion of aerosols in geophysics and in laboratory experiments, *Nonl. Proc. Geophys.* **11**, 343 (2004).
- [32] A. Eidelman, T. Elperin, N. Kleeorin, A. Markovich, I. Rogachevskii, Experimental detection of turbulent thermal diffusion of aerosols in non-isothermal flows, *Nonl. Proc. Geophys.* **13**, 109 (2006).
- [33] A. Eidelman, T. Elperin, N. Kleeorin, I. Rogachevskii and I. Sapir-Katiraie, Turbulent thermal diffusion in a multi-fan turbulence generator with the imposed mean temperature gradient, *Experim. Fluids* **40**, 744 (2006).
- [34] N. E. L. Haugen, N. Kleeorin, I. Rogachevskii and A. Brandenburg, Detection of turbulent thermal diffusion of particles in numerical simulations, *Phys. Fluids* **24**, 075106 (2012).
- [35] T. Elperin, N. Kleeorin and I. Rogachevskii, Mechanisms of formation of aerosol and gaseous inhomogeneities in the turbulent atmosphere, *Atmosph. Res.* **53**, 117 (2000).
- [36] M. Sofiev, V. Sofieva, T. Elperin, N. Kleeorin, I. Rogachevskii and S. S. Zilitinkevich, Turbulent diffusion and turbulent thermal diffusion of aerosols in stratified atmospheric flows, *J. Geophys. Res.* **114**, D18209 (2009).
- [37] A. Hubbard, Turbulent thermal diffusion: a way to concentrate dust in protoplanetary discs, *Monthly Notes Roy. Astron. Soc.* **456**, 3079-3089 (2016).
- [38] J. A. Eastman, S. R. Phillpot, S. U. S. Choi and P. Keblinski, Thermal transport in nanofluids, *Annu. Rev. Mater. Res.* **34**, 219-246 (2004).
- [39] C. Wang, S. K. Friedlander and L. Mädler, Nanoparticle Aerosol Science and Technology: An Overview, *Particology* **3**, 243-254 (2005).
- [40] W. C. Williams, 2007, *Experimental and Theoretical Investigation of Transport Phenomena in Nanoparticle Colloids (Nanofluids)*, (Institute of Technology, Massachusetts, 2007).
- [41] W. Daungthongsuk and S. Wongwises, A critical review of convective heat transfer in nanofluids, *Renew. Sustain. Energy Rev.*, **11**, 797-817 (2007).
- [42] S. Kakac and A. Pramuanjaroenkij, Review of convective heat transfer enhancement with nanofluid, *Int. J. Heat Mass Transf.* **52**, 3187-3196 (2009).
- [43] M. Yu, and J. Lin, Nanoparticle-laden flows via moment method: A review, *Intern. J. Multiphase Flow* **36**, 144-151 (2010).
- [44] M. Lomascolo, G. Colangelo, M. Milanese and A. de Risi, Review of heat transfer in nanofluids: conductive, convective and radiative experimental results. *Renew. Sustain. Energy Rev.* **43**, 1182-1198 (2015).
- [45] M. Raja, R. Vijayan, P. Dineshkumar and M. Venkatesan, Review on nanofluids characterization, heat transfer characteristics and applications. *Renew. Sustain. Energy Rev.* **64**, 163-173 (2016).
- [46] S. M. Vanaki, P. Ganesan and H. A. Mohammed, Numerical study of convective heat transfer of nanofluids: a review. *Renew. Sustain. Energy Rev.* **54**, 1212-1239 (2016).
- [47] T. Elperin, N. Kleeorin, M. A. Liberman and I. Rogachevskii, Tangling clustering instability for small particles in temperature stratified turbulence, *Phys. Fluids* **25**, 085104 (2013).
- [48] M. D. Allen and O. G. Raabe, Reevaluation of Millikan's oil drop data for the motion of small particles in air, *J. Aerosol Sci.* **13**, 537-547 (1982).
- [49] B. V. Derjaguin, A. I. Storozhilova and Ya. I. Rabinovich, Experimental verification of the theory of thermophoresis of aerosol particles, *J. Colloid and Interface Sci.* **21**,

- 35–58 (1966).
- [50] L. Talbot, R. K. Cheng, R. W. Schefer and D. R. Willis, Thermophoresis of particles in a heated boundary layer, *J. Fluid Mech.* **101**, 737-758 (1980).
- [51] H. Chunhong and A. Goodarz A., Particle deposition with thermophoresis in laminar and turbulent duct flows, *Aerosol Science and Technology* **29**, 525-546 (1998).
- [52] G. Santachiara, F. Prodia and C. Cornettia, Experimental measurements on thermophoresis in the transition region, *Aerosol Science and Technology* **33**, 769-780 (2002).
- [53] A. E. Mensch and T. G. Cleary, Measurements and predictions of thermophoretic soot deposition, *Intern. J. Heat and Mass Transfer* **143**, 118444 (2019).
- [54] M. Bukai, A. Eidelman, T. Elperin, N. Kleorin, I. Rogachevskii and I. Sapir-Katiraie, Effect of large-scale coherent structures on turbulent convection, *Phys. Rev. E* **79**, 066302 (2009).
- [55] M. Bukai, A. Eidelman, T. Elperin, N. Kleorin, I. Rogachevskii and I. Sapir-Katiraie, Transition phenomena in unstably stratified turbulent flows, *Phys. Rev. E* **83**, 036302 (2011).
- [56] A. Eidelman, T. Elperin, I. Gluzman, N. Kleorin and I. Rogachevskii, Experimental study of temperature fluctuations in forced stably stratified turbulent flows, *Phys. Fluids* **25**, 015111 (2013).
- [57] L. Barel, A. Eidelman, T. Elperin, G. Fleurov, N. Kleorin, A. Levy, I. Rogachevskii, O. Shildkrot, Detection of standing internal gravity waves in experiments with convection over a wavy heated wall, *Phys. Fluids* **32**, 095105 (2020).
- [58] T. Elperin, N. Kleorin, I. Rogachevskii, Self-excitation of fluctuations of inertial particles concentration in turbulent fluid flow, *Phys. Rev. Lett.* **77**, 5373 (1996).
- [59] T. Elperin, N. Kleorin, V. L'vov, I. Rogachevskii, D. Sokoloff, Clustering instability of the spatial distribution of inertial particles in turbulent flows, *Phys. Rev. E* **66**, 036302 (2002).
- [60] A. Eidelman, T. Elperin, N. Kleorin, B. Melnik and I. Rogachevskii, Tangling clustering of inertial particles in stably stratified turbulence, *Phys. Rev. E* **81**, 056313 (2010).